Military Technical College
Kobry El-Kobbah,
Cairo, Egypt

14th International Conference on
Applied Mechanics and
Mechanical Engineering.

Cylinder Pressure, Performance Parameters, Heat Release, Specific Heats Ratio and Duration of Combustion for Spark Ignition Engine

By

M. S. Shehata*

Abstract:

Experimental study are carried out for investigating cylinder pressure, performance parameters, heat release, specific heats ratio and duration of combustion for multi cylinder spark ignition engine (SIE). Cylinder pressure is measured for gasoline, kerosene and Liquefied Petroleum Gases (LPG) separately as a fuel for SIE at different engine speeds. The engine is coupled by water dynamotor for measuring engine brake power. Fast Fourier Transformations (FFT) are used for transforming measured cylinder pressure from time domain to frequency domain. Empirical correlation is carried out for calculating cylinder pressure in frequency domain for different engine speeds. Inverse Fast Fourier Transformations (IFFT) are used for reconstructing cylinder pressure in time domain. Good agreement between reconstructed and measured cylinder pressure are obtained for different engine speeds. Indicate engine performance parameters are calculated using cylinder pressure measurement. First law-single zone model with γ(T) are used for calculating heat release and heat transfer to cylinder wall. Logarithmic scale of measured cylinder pressure and calculated volume are used for determining polytropic index of compression and expansion processes. Third order correlation for temperature dependant specific heat ratio γ(T) is obtained which is in a good agreement with other researchers. Position of maximum cylinder pressure, maximum temperature and maximum heat release are carried out respectively for different engine speeds. Duration of combustion (Start/end of combustion) for different engine speeds are determined using four different methods: (I) Fuel burned mass fraction, (II) Change of entropy, (III) Temperature dependant specific heats ratio, and (VI) Change of pressure versus cylinder volume in the logarithmic scale. Using entropy change for determining duration of combustion is simple and accurate method. Measurement of engine cylinder pressure is useful tool for understanding the combustion characteristics and determination of reliable statistical data that cannot measured directly. This study is contributed in determining combustion characteristics for different fuels, development and finding optimal operating conditions of multi cylinders SIEs.

Keywords: Cylinder pressure, heat released, duration of combustion, entropy

* Mechanical Engineering Technology Department, Higher Institute of technology Banha University, Egypt

1. Introduction

Cylinder pressure and heat release analysis are important and standard tools for engineers and researchers when developing and tuning new engines. Specific heats ratio model is important for an accurate heat release analysis, where specific heats ratio couples the systems energy to other thermodynamic quantities.

Pin Zeng [1] carried out a new and useful method to reconstruct cylinder pressure for SIE. The only required inputs for cylinder pressure reconstruction using this method are engine speed and load. This method is applied to a 4-cylinder, 2.4-liter DaimlerChrysler SIE. The improved method adds the capability of predicting the effect of engine spark timing on the cylinder pressure. The cylinder pressure can therefore be reconstructed including the third input of spark timing along with speed and load. Comparisons between measured and reconstructed cylinder pressure demonstrate that the method is applicable over the majority of SIE operating range. Reconstructed cylinder pressure traces have also been used to carry out engine heat transfer and heat release analyses.

Nicholas [2] investigated emissions and combustion stability for SIE. Burning rate analysis indicated that the increase in variability for the rapid burning period is greater than that associated with the flame development. Comparisons between the Rassweiler and Withrow approach and a heat release model including heat transfer and blow by terms to calculate the mass fraction burned profile indicated the rapid burn duration was greater with using the heat release approach.

Kamin et. al., [3] Calculated heat release and noise level using cylinder pressure measurement with different spark advance angles. Authors used the time series of heat release to calculate the correlation coarse-grained entropy. The results showed that for a larger spark advance angle the system is more deterministic.

Eriksson and Andersson, (2002) [4] carried out an analytical model for cylinder pressure of SIE. The model takes variations in spark advance and air/fuel ratio into account. Experimental validation on two engines showed that it is possible to describe the cylinder pressure of a SIE operates close to stoichiometric conditions as a function of crank angle, manifold pressure, manifold temperature and spark timing.

Marcus Klein [5] investigated single zone heat release model using $\gamma(T)$. The author computed $\gamma(T)$ for a burned mixture of iso-octane in the temperature range of [500 to 3500] K and pressure range of [0 to 100] bar, which covers most of the closed part of a firing cycle. $\gamma(T)$ is strongly dependent on mixture temperature, air/fuel ratio and pressure. Author found that, for temperatures above 1700 K, the mixture is assumed to be at equilibrium and frozen otherwise. The pressure dependence of γ is only visible for $T>1500$ K and a higher pressure tend to retard the dissociation and yield a higher $\gamma(T)$. The model gave error in order of cylinder pressure measurement noise while keeping the computational complexity at a minimum.

Abu-Nada et. al. [6] used temperature dependant specific heat for cycle analysis of SIE with wide range of engine parameters. The results compared to that used constant specific heats.

In most cases there were significant variations between the results obtained by using specific heats temperature dependence with those obtained at constant specific heats especially at high engine speeds and load due to high temperature variation.

Lanzafame and Messina [7] calculated heat release using the first law-single zone model based on cylinder pressure measurements with assumption of specific heats ratio, wall temperature and polytropic exponent for the motored cycle evaluation. γ(T) has been calculated by new V Order Logarithmic Polynomials (VOLP) and fitting experimental gases properties through the least square methods. The results show that γ(T) has high influences on analysis of heat release.

Jorge et. al. [8] and Bernardo et. al. [9] carried out a model for SIE using the entropy generation minimization method (EGM). Cycle was analyzed and its processes were evaluated by the amount of entropy generated. The main sources for entropy generation are combustion, free expansion, heat transfer, friction and flow through valves. The free expansion and combustion contributed by more than 60% of the entropy generated for all the engine cycles studied. The results also show that the viscous friction of the working fluid inside the engine has no significant impact on the total amount of generated entropy.

Mohand et al. [10] determined the start and end of combustion for SIE from the points of minimum and maximum entropy in the cycle. The end of combustion always matched well with the point of maximum entropy. The start of combustion determined from the rate of change of entropy which showed a sharp change at ignition.

The objective of the present work are using the measured cylinder pressure of SIE with first law-single zone model for analyzing heat release, heat transfer to cylinder wall, γ(T), duration of combustion and reconstructed cylinder pressure using Fast Fourier Transformations (FFT). All parameters are studied using gasoline, kerosene and LPG separately as a fuel at different speeds. The model is carried out using software developed for this purpose with the help of Math Lab soft ware.

2 Experimental Setup

The experimental work has been developed alongside a set of measurements made on a Chevrolet 3.8 litter V-60º engine, six cylinders, 92 mm bore, 84 mm stroke, and compression ratio of 9.25 test system as shown in Fig.(1). A large air box fitted with an orifice plate is used to measure air consumption rate using differential pressure transducer model Setra 239 having differential pressure range of 0-12.7 cm water column with accuracy of 1%. A previous study have confirmed that, the pressure of the air box have negligible effect on the pressure wave in the intake pipe [11]. Cylinder pressure was measured using piezoelectric pressure transducer model Kistler 6123, 0-200 bar as pressure range with sensitivity of 16.5 pc/bar and accuracy of 1.118 %. The accuracy of pressure measurements depends on the pressure transducer, which has a specified non-linearity of less than 1% at full scale.

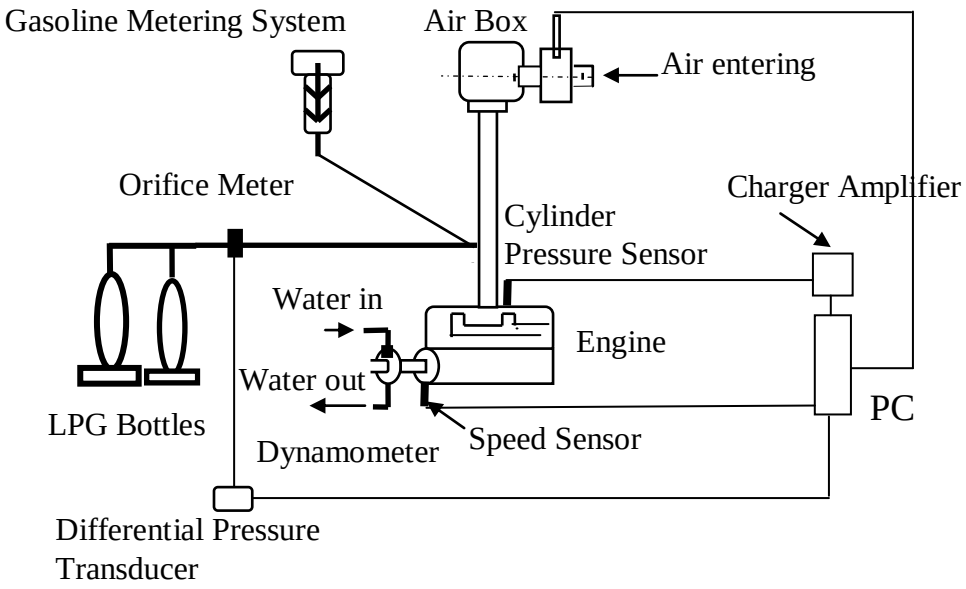

Fig. (1) Experimental Set Up

Charge amplifier model Nexus 6290 was used to process the signal from pressure transducer to a data acquisition card model CIO-DAS1602/12, 12 bit, 32 channel single ended 16 differentials. A slotted disk was fitted to the end of the crankshaft and an optical sensor for measuring engine speed and crankshaft angle position. The liquid fuel flow rate is measured using a fuel volumetric consumption measuring unit model 112116-1-3 with accuracy of ± 0.1 %. LPG fuel is measured with accuracy ± 0.1 % using a calibrated orifice meter with differential pressure transducer model Setra 239. The engine is coupled by water dynamotor for measuring engine torque. The engine is run at various speeds in the range 750-2000 rpm at wide-open throttle and stoichiometric fuel/air ratio. The signals from the pressure and optical sensors were digitised and recorded for later analysis using a data acquisition card and Math lab software. The signal of cylinder pressure is acquired for every 0.1^0 CA and the acquisition process covered 50 completed cycles, the average value of these 50 cycles being outputted the pressure data used for calculation of combustion parameters.

3- RESULTS AND DISCUSSIONS

3.1 Cylinder Pressure Analysis

3.1.1 Cylinder pressure measurement

The cylinder pressure at different engine speeds and different fuels at full wide opening and stoichiometric conditions with firing cases are measured. Due to inability the hydraulic dynamotor to motoring the engine, so cylinder pressure with motored case is calculated and the results are shown in the Figs.(2&3). Cylinder pressure increases with the increase of engine speed up to 1588 rpm due to increase inlet mixture mass flow rate, turbulence intensity and improve mixing process between burned and unburned gases which improves combustion efficiency. For engine speed higher than 1588 rpm the cylinder pressure decreased due to choked flow at inlet valves and this leads to decrease fresh air flow rate.

Cylinder pressure for kerosene fuel is higher than for gasoline and LPG fuels due to high heating value of kerosene compared to that of gasoline and LPG. Also, the burning rate of kerosene fuel is higher than gasoline and LPG fuels. The location of peak pressure for motored pressure occurs at TDC.

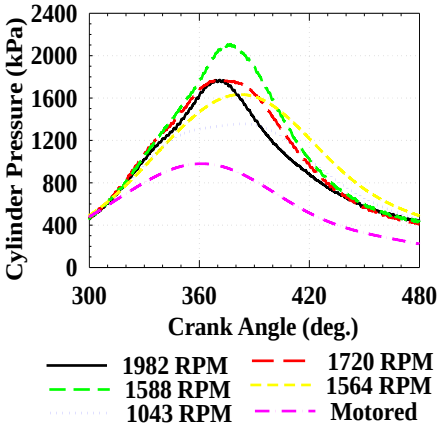

Fig. (2) Cylinder Pressure with Different Speeds at Full Wide Opening and Stoichiometric Air/Fuel Ratio

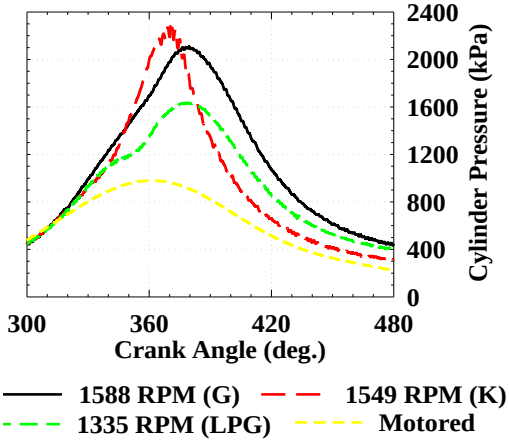

Fig. (3) Cylinder Pressure for Different Fuels with Full Wide Opening and Stoichiometric Air/Fuel Ratio

3.1.2 Fourier Transformation

The Fast Fourier Transformation (FFT) technique is used for transforming cylinder pressures from time domain to frequency domain to carry out empirical correlation for calculating cylinder pressures at different engine speeds in frequency domain. This empirical correlation is used to reconstructed cylinder pressure in frequency domain. Inverse Fast Fourier Transformation (IFFT) is used for transforming cylinder pressure from frequency domain to time domain. So, cylinder pressures are transferred from time domain (crank angle domain) into the frequency domain by FFT technique using the following equations:-

$$P(t) = \overline{P}_{cy} + \sum_{n=1}^{N} [A_n \cos(n\omega t) + B_n \sin(n\omega t)]$$

$$= \overline{P}_{cy} + \sum_{n=1}^{N} C_n \cos(n\omega t + \theta_n) \qquad (1)$$

Where $$C_n = \sqrt{A_n^2 + B_n^2} \qquad (2)$$

$$\theta_n = \arctan(B_n / A_n) \qquad (3)$$

Time-averaged cylinder pressures $\overline{P}_{cy}$ are calculated over complete cycle and the results are stored in Table (1). The amplitude C_n and phase-angle θ_n are calculated using equations (2&3) respectively. The cylinder pressures are decomposed into two curves (the amplitude & phase angle) in the frequency domain. The amplitude curve is normalized by the first harmonic component as follows:-

$$\overline{C_n / C_1} = \{ \sqrt{A_n^2 + B_n^2} \; / \; \sqrt{A_1^2 + B_1^2} \; \} \qquad (4)$$

The normalized amplitudes decreased to less than 0.005 after 40 terms of the Fourier's series. So, only the first 40 terms (N = 40) are used in the analysis. The rest of the terms are neglected and the errors are less than 0.1%.

Figures (4&5) shows the normalized amplitude and phase angles of cylinder pressure using gasoline fuel at 1982, 1720, 1588, 1043 RPM and motored cylinder pressure. The marks in the figure indicate the amplitude and phase angle values as a function of the order of harmonics. The first harmonic component C_1 is proportional to cylinder pressure at different engine speeds. The amplitudes decrease as the order of harmonics increases. When the order of harmonics n>40 the amplitudes C_n decreased to very small values. The normalized amplitude in the frequency domain for different engine speeds has the same order as in the time domain.

The normalized amplitude for 1582 RPM has the highest value while the normalized amplitude for 1988, 1720, 1043 rpm and motored pressure have the lowest values respectively. The phase angle increases with the increase of engine speeds. Because of the turbulence intensity increases the imaginary compound of the amplitude so, the phase angle for 1043 RPM is less than for 1720, 1588 and 1982 RPM due to decrease turbulence with the decrease of engine speed. The data of normalized amplitudes and phase angles for different speeds in the frequency domain are combatable with that in the time domain. The phase angle decreases with increased order of harmonic because the sine wave components (Imaginary components) for the cylinder pressure are fewer. The turbulence intensity increases with the increase of engine speed and the turbulence creates irregular wave components (Imaginary components) in engine cylinder. These turbulence induced components have higher frequencies, which gives a low contribution at high order of harmonics and a larger one at lower order of harmonics. Hence, the normalized amplitude decreases with the increase of harmonics order. After n>20, the amplitudes of cylinder pressure drop close to zero, and phase angles are stilled increase. Based on the present data, the phase angle curves are nearly straight lines for different engine speeds. The linear feature of the phase angle at different order of harmonics can be used to simplify the calculation and minimize the data volume that need to be stored. The present analysis of the cylinder pressure waves in the frequency domain is useful for determining the noise intensity, the magnitude/direction of the pulsating forces inside engine cylinder especially at detonation conductions.

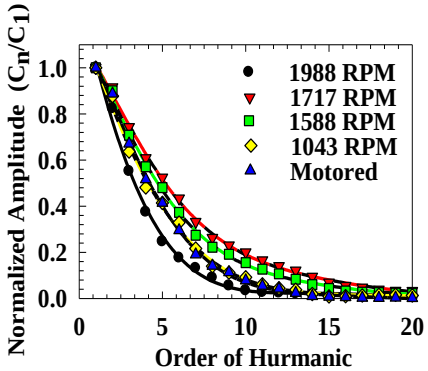

Fig. (4) (C_N/C_1) of Cylinder Pressure in Frequency Domain for Gasoline Fuel with Different Engine Speeds

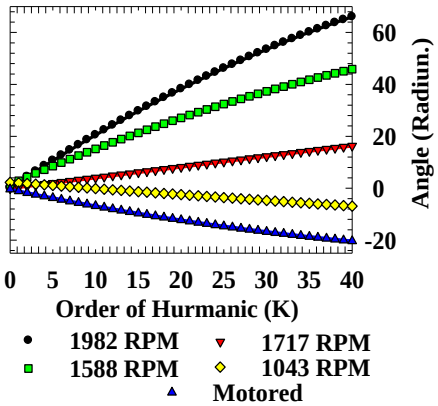

Fig. (5) Phase Angle of Cylinder Pressure in Frequency Domain for Gasoline Fuel with Different Engine Speeds

Figure (6&7) shows the normalized amplitude and phase angles of cylinder pressure for different fuels. The normalized amplitudes in the frequency domain for different fuels have the same order and combatable with that in the time domain. At begaining of combustion gasoline has higher magnitude than kerosene and LPG fuels. At end of combustion kerosene has higher magnitude than gasoline and LPG. These values are combatable with their values in time domain. The phase angle for gasoline fuel is greater than for kerosene and LPL due to gasoline has higher imaginary component than kerosene and LPG.

For different engine speeds, time-averaged cylinder pressure $\overline{P}_{cy}$ and the first order harmonic component C_1 are stored in table (1) for reconstructing cylinder pressure at different engine speeds. The cylinder pressures waves are of a periodic nature and by examining the Discrete Fourier Transform of pressure wave, an accurate reconstruction of cylinder pressure waves are created. These are made by calculating amplitudes and phase angles in the frequency domain and then used to reconstruct the pressure waves in time domain. The main advantage of using the frequency domain is the pressure wave can be accurately described using only a few frequencies. All the phase angle curves start from the same point, so the phase angle values at the second point (second harmonic) for each curve are determined and stored in table (1) for later used in reconstructed cylinder pressure at different engine speeds. Also, representative values of θ_N for all curves are found and stored in Table (1). The ending values θ_N (θ_n at n = N) are spread over a wide range. Because θ_N values change with engine speed in an irregular pattern, so, it is difficult to find a parameter to normalize them. Therefore, their values are stored in Table (1). All phase angles are nearly straight lines, these lines are defined by the following equation:-

$$\frac{\theta_n - \theta_2}{n-2} = \frac{\theta_N - \theta_2}{N-2}$$

$$\text{OR} \qquad \theta_n = \theta_2 + \{(n-2)/(N-2)\}(\theta_N - \theta_2) \qquad (5)$$

Averaging the normalized amplitude $\overline{C_n/C_1}$ values for different engine speeds as a function of the order of harmonics n (n = 1, 2 … N), a mean normalized amplitude curve $\overline{C_n/C_1}$ is generated and fitted into a polynomial equation. In the present work, an 8th order polynomial equation is used to curve fit the data for later use in reconstructing the cylinder pressures.

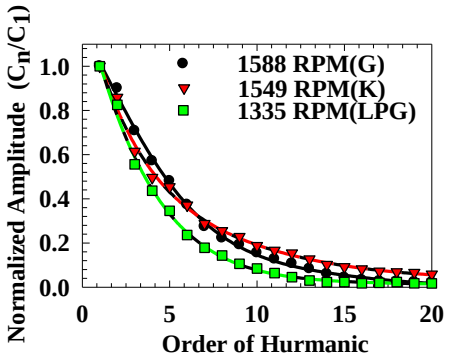

Fig. (6) (C_N/C_1) of Cylinder Pressure in Frequency Domain for Different Fuels

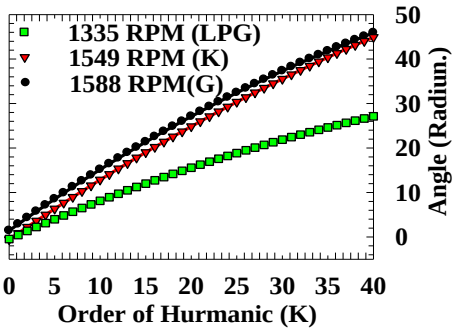

Fig. (7) Phase Angle of Cylinder Pressure in Frequency Domain for Different Fuels

3.1.3 Data Processing and Fitting

Now all the data needed for reconstructing cylinder pressures have been calculated and stored in Table (1) and fitted into equation (6) for reconstructing cylinder pressure as follows:-

$$\overline{C_n/C_1} = 1.2120 - 0.1954n - (9.9542E-4)n^2 + (2.6998E-3)n^3 - (2.8472E-4)n^4 + (1.4317E-5)n^5 - (3.9221E-7)n^6 + (5.6250E-9)n^7 - (3.3087E-11)n^8 \quad (6)$$

$$\text{Where} \quad (n = 1,2,3,\ldots\ldots\ldots N)$$

In the next step, these values and equation (1) will be used to reconstruct the cylinder pressures waves at different engine speeds. The process of reconstructing cylinder pressures at the tested points is the reverse of the above steps. Directly using data stored in Table (1) as well as equations (6) and equations (1,2,3&4) the cylinder pressures can be reconstructed for all operating speeds. Note that the proposed method for reconstructing cylinder pressure does not alter either the time-averaged cylinder pressure or its first harmonic component for the test speeds. The measured and reconstructed cylinder pressures at engine speeds of 1043, 1564, 1588, 1720 and 1982 rpm are shown in Fig (8&9). From the results, it can be observed that good agreement between the measured and reconstructed cylinder pressure. This is attributed to the fact that the normalized amplitude $\overline{C_n/C_1}$ as a function of order of harmonic falls into a narrow range, but does not collapse into a single curve.

Table (1) Time average cylinder pressures $\overline{P}_{cy}$ (bar), the first order Harmonic components C_1 (bar) and phase angle θ_2 and θ_N (radian)

Engine Speed (RPM)	Gasoline			
	($\overline{P}_{cy}$) bar	C_1 (bar)	phase angle (Radian)	
			θ_2	θ_N
1982	3.687681	2834.6923	2.2563	4.1893
1720	3.554825	3825.2000	2.7707	5.7259
1588	3.846097	4226.7023	2.8819	2.1359
1043	3.661886	7220.1204	2.0390	3.4667
Motored	1.859701	2547.2412	-1.0739	0.6822
Kerosene				
1549	3.619550	3938.2661	**0.8596**	**4.6459**
LPG				
1335	3.712052	4485.5527	0.4465	4.2222

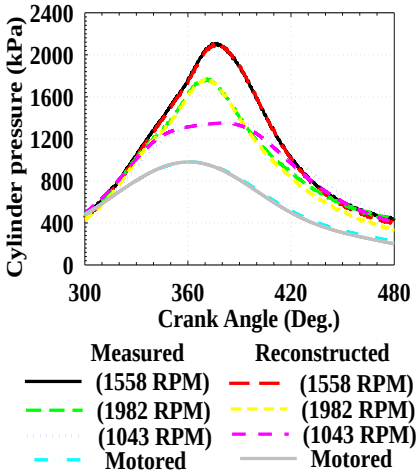

Fig.(8) Comparision between Measured and Reconstructed Cylinder Pressure for Gasoline Fuel at Different Speeds

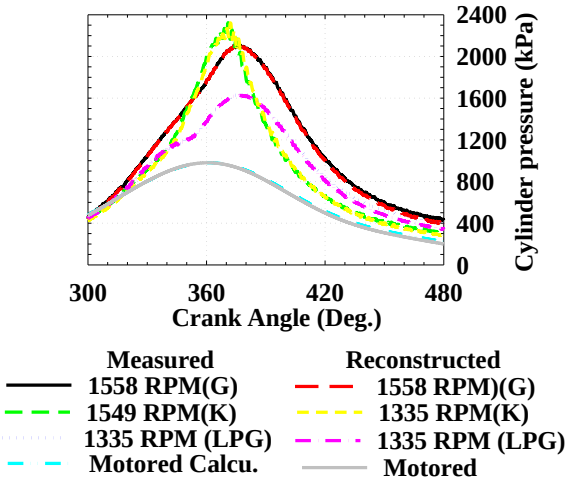

Fig.(9) Comparision between Measured and Reconstructed Cylinder Pressure for Different Fuels in Time Domain

3.2 Engine performance Parameters

Indicate mean effect pressure (IMEP), pumping mean effect pressure (PMEP), indicate power (IP), brake power (BP), indicate specific fuel consumption (ISFC), indicate thermal efficiency (η_{th}), volumetric efficiency (η_V), mechanical efficiency (η_m)} were calculated using the measured cylinder pressure. The model equations were found in [12]. The calculated and the measured engine performance parameters are drawn verses IMEP as shown in Figs.(10&11). All engine performance parameters are compatible with each other. The performance parameter are varied between: η_V(55 to 65)%, η_V(70 to 80)%, η_{th}(20 to 26)%, BP(12 to 33) kW, ISFC(0.37 to 0.82) kg/kW-hr, IMEP(1 to 9) kW and PMEP (20 to 40) kPa. All the obtained data for engine performance parameters are within the acceptable range. From reconstructed cylinder pressure and evaluation of performance parameter the development and optimum operating conditions for SIE can be determined.

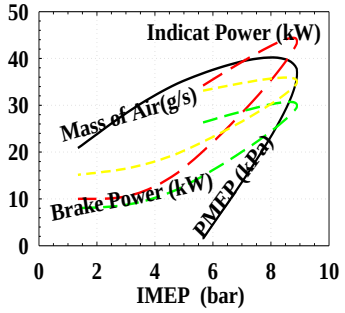

Fig. (10) Engine Performance Parametres for Gasoline Fuel at Full Throttling and Stoichiometric Air/Fuel Ratio

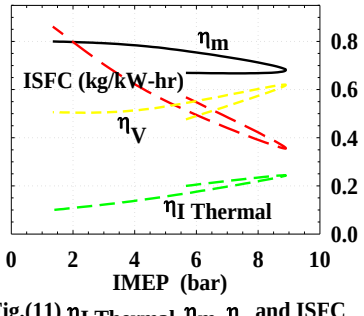

Fig.(11) $\eta_{I\ Thermal}$, η_m, η_V and ISFC for Gasoline Fuel at Full Throttling and Stoichiometric Air/Fuel Ratio.

Engine torque mainly consist of two group, the basic torque describes mass and gas forces working on the crank shaft outside the combustion process, while the indicate torque mainly deals with gas forces during combustion process. Author intensity deals with indicate torque

for different engine speeds and fuels and the results are shown in Figs.(12&13). The instantaneous torque $T_i(\theta)$ due to combustion is obtained through the absolute pressure in the cylinder $P_{cyl}(\theta)$ and the counteracting pressure on the back of the piston P_0 as follows:-

$$T_i(\theta) = [P_{cyl}(\theta) - P_o] - A_p(dZ/d\theta) = (P_g)A_p(dZ/d\theta)$$

$$\text{and} \quad \frac{dZ}{d\theta} = [\, L_{ct}\sin\theta\,](1 + \frac{L_{ct}\cos\theta}{\sqrt{L_{cr}^2 - (L_{ct}\sin\theta)^2}}) \qquad (7)$$

Before the end of the cycle, it can be seen that the torque increases a bit. This is when the inlet valve opens and the flow of air between the two manifolds, through the cylinder, creates a short but positive work on the piston. Then as the piston reaches TDC, it turns and produces a negative torque as it is pulled down by the rotation of the crankshaft. The pressure then rises as more air enters the cylinder, and the torque turns positive. At 180± the compression stroke begins and the torque reaches the lowest point of the cycle as plenty of work is needed to compress the air within the cylinder. Shortly before ±360, fuel is ignited producing positive work characterized by the peaking torque curve. Then at ±540 the exhaust stroke begins and the torque becomes negative since work is needed to push the exhaust gas out of the cylinder. The indicate torque are combatable with cylinder pressure for different engine speeds. Maximum effective torque for LPG is greater and delayed ATDC than that for gasoline and kerosene respectively due to low burning velocity. The torque increases with increasing engine speed since the torque would rather decrease in order to maintain the power of the engine. One possible explanation can be found in the wall-heat losses during the high pressure loop covered by the effective torque. These losses decrease with increasing engine speed and thereby alter the power output of the engine.

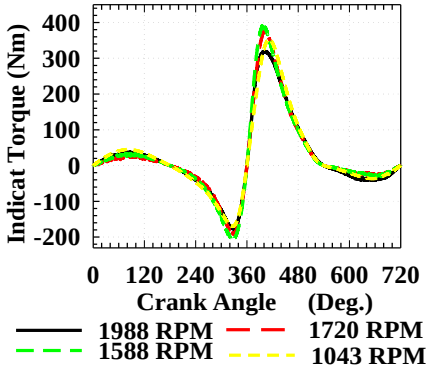

Fig.(12) Indicated Torque for Gasoline with Different Speeds at Full Wide Opening and stoichiometric conditions

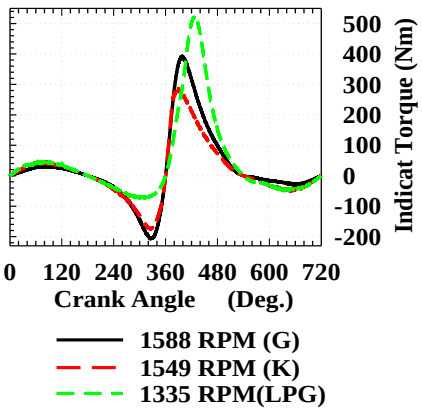

Fig.(13) Indicated Torque for Different Fuels at Full Wide Opening and stoichiometric

3.3 Heat Release and Heat transfer Models

Heat release, heat release rate dQ(θ)/dθ and heat transfer to cylinder wall are major parameters will be calculated using the measured cylinder pressure P(θ). Engine cylinder volume (V) and the change of cylinder volume (dV/dθ) as function of crank angle θ are calculated as follows:-

$$V = [\ L_{cr} + L_{ct}(1 - \cos\theta) - \sqrt{L_{cr}^2 - (L_{ct}\sin\theta)^2}\ ]\ \{\frac{\pi B^2}{4}\} + V_c$$

$$\text{and} \quad \frac{dV}{d\theta} = \{\frac{\pi B^2}{4}\}[\ L_{ct}\sin\theta\ ](1 + \frac{L_{ct}\cos\theta}{\sqrt{L_{cr}^2 - (L_{ct}\sin\theta)^2}}) \qquad (8)$$

The pressure change with respect to crank angle ($dP/d\theta$) is calculated from cylinder pressure measurement as function of crank angle θ as follows:

$$\frac{dP}{d\theta} = \frac{P_{i+1} - P_{i-1}}{\theta_{i+1} - \theta_{i-1}} \qquad (9)$$

For internal combustion engine the combustion process is occurred after inlet valve closed (IVC) and before exhaust valve opened (EVO) so, the first law of thermodynamics, for closed systems is used for calculating the heat release as follows:-

$$dQ - dW = dU \qquad (10)$$

Where $dW = -PdV$, $dU = m\,C_v(T)\,dT$, $dT = d(PV)/mR$, and $R/C_v(T) = \gamma(T) - 1$

The total mass m and gas constant R are assuming to be constant during the combustion process. These assumptions are reasonable since the molecular weights of the reactants and the products are essentially the same. After rearranged the above terms, the gross heat release rate is calculated as follows:-

$$\frac{dQ_{HR}}{d\theta} = \frac{\gamma(T)}{\gamma(T) - 1} P \frac{dV}{d\theta} + \frac{1}{\gamma(T) - 1} V \frac{dP}{d\theta} + \frac{d\dot{Q}_{wall}}{d\theta} \qquad (11)$$

Several parameters are presented in the mathematical model for the gross heat release rate evaluation. The specific heats ratio γ(T) has a great influence on shape and peak of the heat release trace [13]. First law-single zone model for the heat release rate with γ(T) is developed. This model has many advantages, (I) It describes with accuracy the physic of the phenomenon (charge heat release during the combustion stroke and heat exchange between gases and cylinder wall), (II) It has a great simplicity in the mathematical formulation, and (III) The implementation of γ(T) function reduces notably the error deriving from a wrong choice of the constant value of γ. The γ(T) of the gases is calculated using equation produced from experimental data of [13]:

$$\gamma(T) = 1.338 - 6(E\text{-}5)T + 1(E\text{-}8)T^2 \qquad (12)$$

A low value of specific heats ratio produces high value of heat release and a heat release rate that is negative after the completion of combustion. The heat transfer from gases to cylinder wall is taken into consideration to calculate gross heat release rate. The heat transfer modeling error does not affect the cylinder pressure immensely [5]. There are many models for heat transfer coefficient (h_C). The most widely used is proposed by [14].

$$h_C = 129.8 B^{0.2} P^{0.8} T^{-0.55} w^{0.8} \qquad (13)$$

Woschni [14] stated that the characteristic speed w depends on two terms. One is due to piston motion and is modeled as the mean piston speed $\bar{S}_P$. The other term is due to swirl originating from the combustion event, which is modeled as a function of the pressure rise due to combustion, i.e. ($P - P_0$). The charge velocity w due to piston motion and due to combustion process is expressed as follows:-

$$w = C_1\bar{S}_P + C_2(T - T_0) = C_1\bar{S}_P + C_2\frac{V_d T_r}{P_r V_r}(P - P_{motored}) \qquad (14)$$

Where the first term originates from convection causes by piston motion and the second term from the combustion itself, where T_0 is the motored mean gases temperature. All thermodynamic states (P_r, T_r, V_r) are evaluated at a given reference condition such as IVC (P_{IVC}, T_{IVC}, V_{IVC}). T_{ivc} and P_{ivc} are temperature/pressure at IVC and equal 330 K, $1.013x10^5$ Pa. The constant C_1 and C_2 are listed in table (2). Woschni [14] stated that the parameters (C_1, C_2) are engine dependent and therefore change for different engines geometries. The heat transfer correlations do not have a significant influence on the engine performance prediction. Typically, a 10 % error in the prediction of in-cylinder heat transfer leads to an error in the order of 1 % for the engine performance [5].

Table (2) C_1 and C_2 Values

Process	C_1	C_2
Gases exchange	6.18	0.0
Compression	2.28	0.0
Combustion and expansion	2.28	3.24x!0^{-4}

The motored pressure at specific crank angle θ is calculated as follows: -

$$P_{cyl.motored}(\theta) = \beta P_r\left(\frac{V_{cyl}}{V_r}\right)^{\gamma} \qquad (15)$$

Where β is a constant in a range of 0.5 to 0.7

The rate of heat transfer from gases to cylinder wall is calculated as follows:-

$$\dot{Q}_w = A(\theta)_{cy}\, h(T - T_W) \qquad (16)$$

The instantaneous combustion chamber surface area A(θ) is calculated as Follows:-

$$A(\theta)_{cy} = A_{ch} + A_{pc} + A_{lat}(\theta) \qquad (17)$$

Where A_{ch} is the cylinder head surface area and A_{pc} is the piston crown surface area. For flat-topped pistons, $A_{pc} = (\pi/4)(B)^2$. The lateral surface area $A_{lat}(\theta)$ is approximated by the lateral surface of a cylinder, and A_{ch} is assumed to be equal to A_{pc}. The instantaneous combustion chamber surface area can then be expressed as follows:-

$$A(\theta)_{cy} = \{\frac{\pi B^2}{2}\} + (\pi B)[\,(L_{cr} + L_{ct}) - (L_{ct}\cos\theta) - \sqrt{L_{cr}^2 - (L_{ct}\sin\theta)^2}\,] \qquad (18)$$

With the help of measured cylinder pressure and the calculated cylinder volume, the gases temperature T is calculated using equation of state as follows:-

$$T = \frac{T_r}{P_r V_r} PV \qquad (19)$$

The gases temperature as a function of crank angle degrees for different engine speeds with different fuels are shown in Figs.(14&15). The gases temperature increases drastically at the beginning of combustion. After that its decreases due to the decrease of heat release rate with diminishing amount of fuel burning and expansion causes by the piston movement. The gases temperature increases with the increase of engine speed up to 1588 rpm due to increase cylinder pressure and turbulence intensity. For low engine speed of 1043 rpm at the beginning of combustion the gases temperature is low due to low turbulence and lake of burning rate. Near end of combustion the low engine speed has the highest gases temperature due to more amount of fuel burnt. When engine speed increased from 1043 to 1588 the maximum gases temperature reduced from 2400 K to 2200 K, and it is occurred 5°CA later. As the engine speed increased from 1588 rpm to 1982 rpm maximum gases temperature increased from 2500 K to 2660K and occurred at 20°CA earlier. The peak gases temperature position at engine speeds of 1043, 1588 and 1981 are 43°, 38°, and 42° deg ATDC respectively.

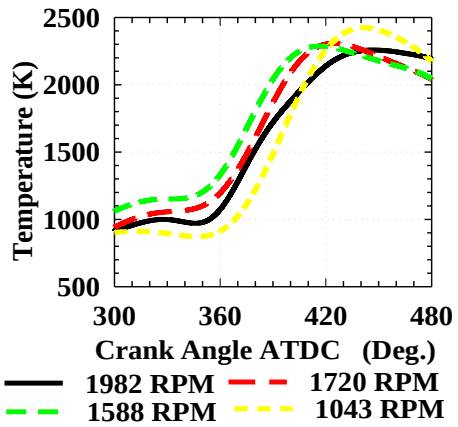

Fig.(14) Gases Temperature for Gasoline Fuel with Different Speeds at Full Wide Opening

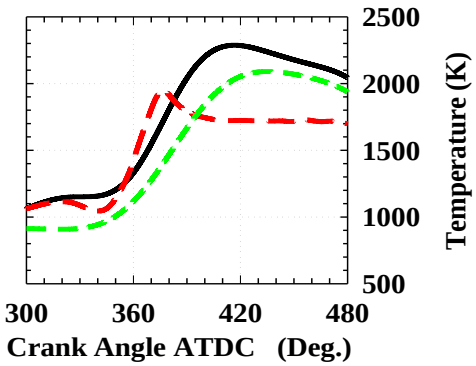

Fig.(15) Gases Temperature for Different Fuels at Full Wide Opening

The variation in the crank angle cross bonding to the peak gases temperature reflects the longer combustion duration (as crank angle) with the increase of engine speed. At low engine speed, combustion duration (as a time) increases due to reduce flame speed. The peak gases temperature for gasoline is higher than for LPG and kerosene fuels respectively. The position of peak gases temperature for kerosene fuel is earlier than for gasoline and LPG fuels respectively. So, heat losses to cylinder wall for kerosene is higher than for gasoline and LPG fuels respectively. The rate of increase and the rate of decrease of gases temperature for kerosene are steeper than for gasoline and LPG due to kerosene has the higher fuel burning rate. The position of peak temperature for LPG is later than gasoline and kerosene fuels due to lower flame speed and fuel burning rate.

The gross heat released rate is calculated using equations (7 to19). The net heat release rate at engine speed of 1982 rpm for different values of γ is shown in Fig.(16). Also, the net heat release rate for different fuels and γ equal 1.35 is shown in Fig.(17). Net heat release rate for different engine speeds and different fuels with γ(T) are shown in Figs.(18 & 19), also, gross heat release rate are shown in Figs.(20&21).

The net heat release rate increases with the decrease of γ due to increase gases temperature. For low γ heat release is too high and negative after end of combustion. Maximum net heat release for gasoline is higher than for LPG and kerosene fuels respectively. The position of maximum net heat release for gasoline is delayed than that for kerosene and LPG respectively. The net heat release rate with γ(T) coincide with the constant specific heats ratio at γ = 1.25. Changing engine speed or engine fuel the exact value of γ will be varied and the correct value needs high level of experiences. Utilizing γ (T) it is possible to avoid this typology of error. As γ decreases, the position of maximum net heat release is more delayed ATDC due to high heat generation. From comparison Figs.(14&15) it is possible to notice that γ has high influence on maximum net heat release rate. So, for a correct evaluation of the heat release rate it is necessary to use γ(T). The net heat release profile decreases during the part of the cycle due to the heat transfer to walls. After that a rapid increases due to combustion and the conversion of chemical energy to thermal energy. Finally, the trend is steeper decreasing after combustion than before combustion due to high heat losses with higher temperature and turbulence intensity. Turbulence is an important factor for efficient combustion because it affects the mixing of air, fuel and residual gases. The net heat release rate demonstrates the significant increase in combustion rate with the increase of engine speed.

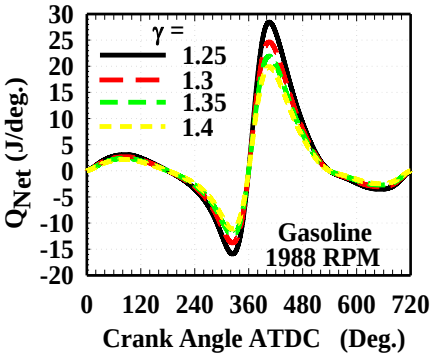

Fig.(16) Net Heat Release Rate for Gasoline at 1988 RPM with Different values of γ

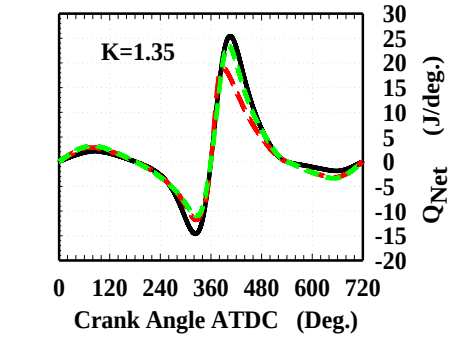

Fig.(17) Heat Released Rate for Different Fuels with Polytropic Index 1.35

From comparing Figs.(18&20) and Figs.(19&21), the net and gross heat release rates for different speeds and different fuels have the same trends but with different numerical values. The gross heat release is greater than the net heat release due to addition heat transfer term. Engine speed corresponding to maximum cylinder pressure has maximum net and gross heat release rates due to maximum flame temperature. So, engine speed of 1588 rpm has highest net and gross heat release rates. The other speeds have net and gross heat release rates depend on the values of cylinder pressure relative to maximum cylinder pressure at 1588 rpm. The increase in the net heat release rate is the reason for decreasing combustion

duration. The heat release rate at a high engine speed is quite wavy in nature showing the poor combustion stability. At high engine speed, the heat release and combustion rates increase due to increase turbulence intensity. Also, combustion is completed earlier at high engine speed due to increase flame speed. On the other hand, at low engine speed the heat release extends in the exhaust stroke carried out more unburned hydrocarbon due to lack burning velocity and heat liberation. From Fig.(19), the maximum net heat release rate for gasoline is higher than for LPG and kerosene respectively due to gasoline has density which means higher mass for the same swept volume. The position of maximum net heat release rate for kerosene is earlier than gasoline and LPG respectively due to higher burning velocity than gasoline and LPG respectively.

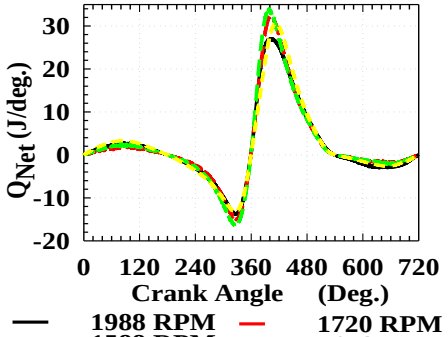

Fig.(18) Q_{Net} for Gasoline with Different Speeds and γ(T)

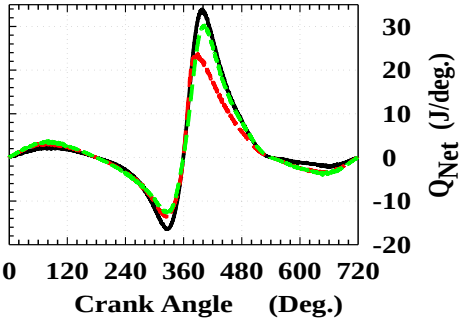

Fig.(19) Q_{Net} for Different Fuels and γ(T)

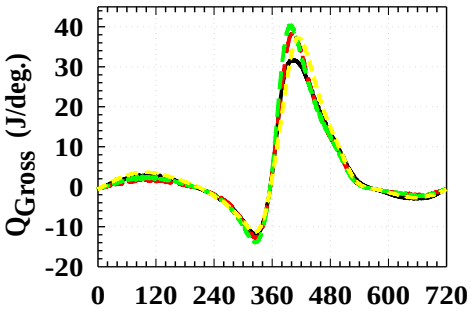

Fig.(20) Q_{Gross} for Gasoline with Different Speeds and γ(T)

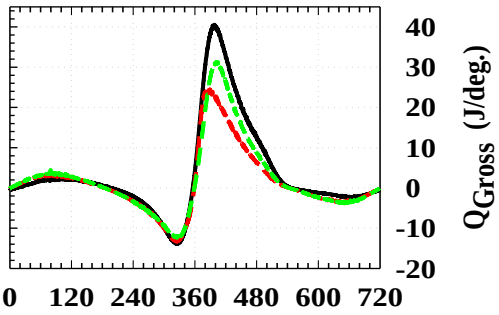

Fig.(21) Q_{Gross} for Different Fuels and γ(T)

Furthermore, The heat flux to cylinder wall for different engine speeds and different fuels are shown in Figs.(22&23). The heat flux for different engine speeds is related to cylinder pressure and gases temperature. Position of maximum heat flux for the higher engine speed is the earlier than the other speeds. Maximum heat flux for kerosene fuel is greater than for gasoline and LPG. Position of maximum heat flux for kerosene is earlier than gasoline and LPG respectively. The heat flux in the suction process is negative for all operating conditions due to heat transfer from cylinder wall to fresh charge where wall temperature is higher than fresh charge. At the end of exhaust process after IVO during over lab angle the heat flux is

also negative due to the heat transfer from wall to fresh charge. Most of heat flux to walls is occurred in the combustion and exhaust processes for different operating conditions where gases temperature is higher than wall temperature. LPG fuel has less heat flux than other fuels due to less carbon/hydrogen ratio than gasoline and kerosene where carbon increases heat flux by radiation from hot spot to different areas in cylinder walls.

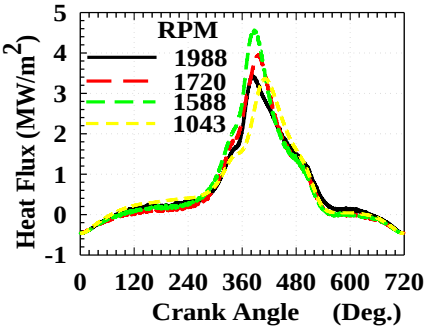

Fig.(22) Heat Flux to Cylinder Wall Using Gasoline at Different Speeds

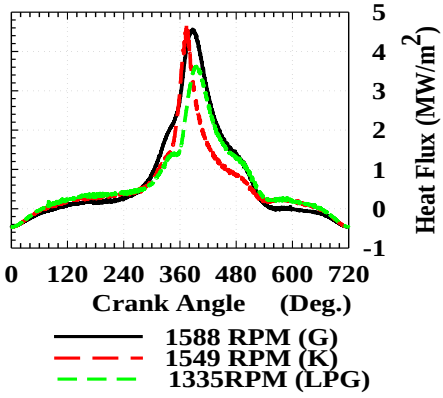

Fig.(23) Heat Flux to Cylinder Wall for Different Fuels

3.4 Specific Heats Ratio γ(T)

The use of log (pressure) versus log (volume) plots provides a direct way to determine start and end of combustion. Such a plot obtained using cylinder pressure measurement at different engine speeds and different fuels as shown in Figs.(24&25). In the log-log scale, the slope is the polytrophic coefficient. The polytrophic coefficient for the compression process is excellent where the process is straight line to end of compression process. For the expansion process it is slightly small due to the end of combustion process is different for different engine speeds, different fuels used, and engine operating conditions. Also, the polytrophic coefficient depends on engine operating point and it is also different for engine type and design. The compression and expansion processes are nearly straight lines indicating that the corresponding polytropic exponents are almost constant. The start and end of combustion are determined where the trend deviates from a linear behavior for compression and expansion processes. These points have to be located with care by drawing tangents to the compression and expansion processes. From comparison P-V diagram for different engine speeds, the author concludes that, the duration of combustion as a crank angle increases with the increase of engine speed. The area enclosed by the cycle processes gives the net work given by the cycle. The area enclosed on P-V diagram for engine speed of 1588 rpm is higher than for 1982, 1720 and 1043 rpm respectively. This means that for engine speed of 1588 rpm the net work given by the cycle is higher than other speeds. The area enclosed on P-V diagram for gasoline fuel is greater than for LPG and kerosene respectively. So, for gasoline fuel the engine gives higher net work than for LPG and kerosene respectively. From comparison P-V diagram for different fuels the author concludes that the duration of combustion for kerosene is smaller than for gasoline and LPG respectively.

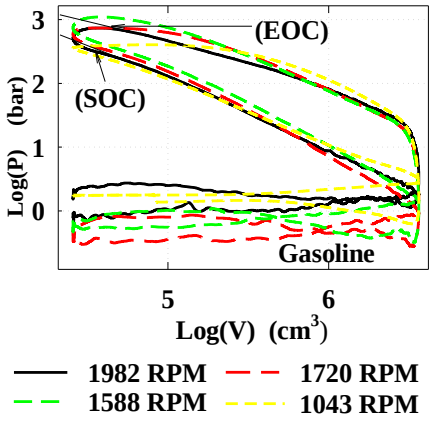

Fig.(24) Pressure Versus Cylinder Volume for Gasoline at Different Speeds

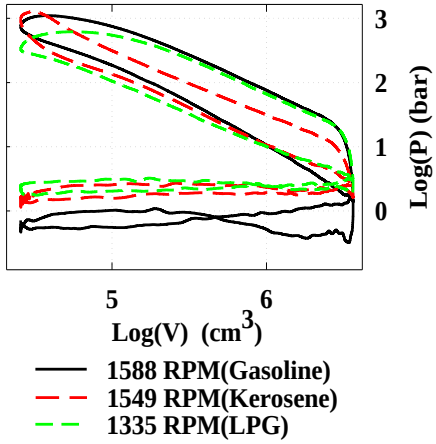

Fig.(25) Pressure Versus Cylinder Volume for Ddifferent Fuels

An accurate specific heats ratio model is important for an accurate heat release analysis due to the specific heats ratio couples the systems energy parameters to other thermodynamic quantities. The objective of this section is to carry out correlation for γ(T). γ(T) is calculated as (log(ΔP)/log(ΔV)) for different engine speeds and different fuels. γ(T) using equation (12) and γ(T) based on log(ΔP)/log(ΔV) for different engine speeds and different fuels are carried out and the results are shown in Figs.(26&27). γ(T) traces have the same trends for both cases but with different numerical values. γ(T) for different speeds and different fuels are related to gases temperature. Specific heats ratio based on log-log scale is nearly 1.175-1.33 for different operating conditions and γ(T) is nearly 1.25-1.33 for different temperature range. The specific heats ratios for both cases decrease with the increase of gases temperature. For both cases specific heats ratios have nearly the same values in all cycle processes except in the combustion process where there is some deviation between the two methods due to the log-log scale in this process is not straight line and is a higher order.

Furthermore, the specific heat traces based on log(ΔP)/log(ΔV) scale are used for determining start and end of combustion. In compression process where wall temperature is higher than mixture temperature and heat transfer from wall to gases so, specific heats ratio decreases up to start of combustion where gases temperature is higher than the wall temperature. This point is the inflection point in the specific heats ratio traces based on log(ΔP)/log(ΔV) where the traces change from increase to decrease. In the combustion process the heat transfer from gases to cylinder wall and so, the specific heats ratio decreases. At the end of combustion where there is no heat generated and the heat transfers from cylinder wall to combustion gases. This point for specific heats ratio based is the second inflection point and is the corresponding to end of combustion. From the two inflection points duration of combustion are carried out for different engine speeds and different fuels. Using specific heats ratio method for determining start and end of combustion has many advantages, (I) Accurate method depends on actual cylinder pressure measurements and not include any assumptions as in the other computational models., (ii) This computational efficiency of course comes to a cost of less descriptive models., (iii) The method gives indications to start and end of heat transfer from cylinder gases to cylinder wall and vice versa., This is a good method for determining start and end of combustion at different operating conditions. The method is valid for any application and it needs only to gases thermodynamics properties and directly valuable from experimental pressure measurements.

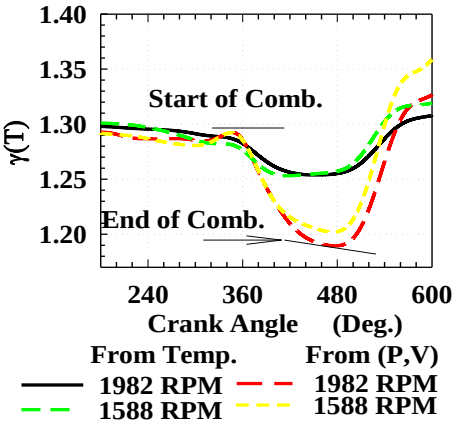

Fig(26) Comparison between γ(T) Calculated from T_{Gas} and Calculated from (log P/log V) for Different Speeds

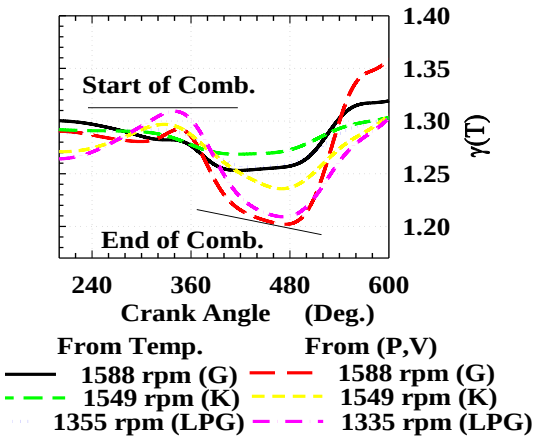

Fig(27) Comparison between γ(T) Calculated from T_{Gas} and Calculated from (log P/log V) for Different Fuels

The specific heats ratio during the closed part of the cycle is frequently modeled as either a constant, or as a linear function of temperature **Gatowski et al. [15].** This model can be written as follows:

$$\gamma(T)_{lin} = \gamma(300) + b\,(T - 300) \qquad (20)$$

The results are dependent on the slope b and constant γ(300). In temperature range of (500 - 7000 K), γ(300) equal 1.3695 and b equal (-9.6E-5). γ(T) polynomial model is more accurate than second order and the linear models, since the normalized root mean square error (NRMSE) is smaller. For the present work γ(T) based on log(ΔP)/log(ΔV) scale is calculated for different operating conditions and plotted versus gases temperature. After that one curve is fitted for different speeds and different fuels to get the general equation for γ(T) as follows.

$$\gamma(T) = 1.3926 - 1.0718(10^{-4})T - 2.127(10^{-8})T^2 + 1.3814(10^{-11})T^3 \qquad (21)$$
$$(\ 298\,K < T < 2200\,K)$$

The present equation based on log(ΔP)/log(ΔV) scale and Brunt equation [13] , Gatowski [15] , and results of Marcus [5] for γ(T) are plotted versus gases temperature as shown in Fig.(28). The intersection of different models are nearly at γ equal 1.29 which is nearest to the constant value of γ which gave the same heat release rate for three cases (constant value of γ, using Brunt equation and γ based on log(ΔP)/log(ΔV)). Good agreement between the present results and Marrcus results in all temperature range. At gases temperature above 1800 K there is some deviation between the present and Marrcus results and Gatowski results. The difference between Brunt equation and the other results (the present, Marrcus and Gatowski results) is not exceeded ±2.7% which is good agreement for engineering applications. All models gave the value of γ in the suitable range of 1.2 to 1.4 for all temperature ranges excepts for Gatowaki which gives less value at gases temperature higher than 1800 K. The slightly difference between different models can be attributed to the

experimental data of cylinder pressure for different operating conditions and different fuels. The root mean square error for the cylinder pressures measurements is in the range of ± 3% and the cylinder pressure measurement has direct effect on values of γ(T) for the single-zone model. So, it is necessary to evaluate accurate values of cylinder pressure and γ(T). The modeling error of heat release is dependent on the accuracy of measuring cylinder pressure and calculating γ(T). The linear and second order models of γ(T) introduce a modeling error in cylinder pressure calculation which is 15 times the cylinder pressure measurement noise. The present equation carried out an alternative, simple and direct method for the calculation of γ(T) function. The method is valid for any application and it needs only cylinder pressure measurements.

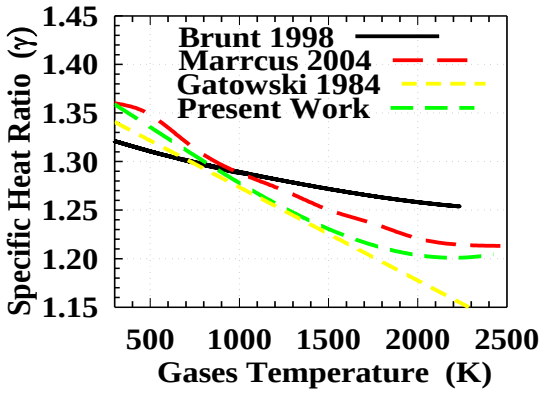

Fig(28) Comparison between γ(T) from Previous Researchers and γ Fitted from (log P/log V) (Present)

3.5 Duration (Start and End) of Combustion

The analysis of the cylinder pressure versus crank angle data yields information on the starting and ending of the combustion processes. It is well known that these parameters have a significant influence on the thermal efficiency and peak cylinder pressure of an engine. Three methods for determining the start and end of combustion will be analyzed.

1- The use of log (P) versus log (V) plot provides a direct way to determine start and end of combustion as shown in Figs.(24&25).
2- The used of two inflection point of specific heat ratio as shown in Figs.(26&27).
3- The mass fraction of fuel burnt is determined using Wiebe function method. The model equations are found in Heywood [12] and the results are shown in Figs. (29&30).
4- The used of crank angle for minimum and maximum gas entropy as shown in Figs.(31&32).

The mass fraction burned curves varied dramatically and the greatest variation appears to be at the start of combustion. The start of combustion ranges from about 340 to 360 crank angle degrees. Burn duration is slightly decreased by the increase in pressure at the spark. In actuality, an increase in the initial pressure during combustion can greatly alter the way of fuel burns. Higher pressure in a limited volume means that the temperature in the cylinder is higher and that the fuel and air molecules are more reactive. The mixture burns faster, so the burn duration becomes shorter. The delayed spark firing takes advantage of the more reactive nature of the fuel to get more power out of the stroke. Under high pressure, the

gases in the cylinder are hotter throughout combustion which is an oxidation reaction and occurs faster. This increase in reaction rate is due to the increased kinetic energy so it takes a smaller amount of additional energy to reach the activation energy for the reaction. At any crank angle position, percentage of fuel burning for LPG fuel is less than for gasoline and kerosene fuels due to decrease fuel burning velocity. This means that, fuel burning rate of kerosene is higher than for gasoline and LPG fuels. The mass fraction burning curve for LPG is less steep than gasoline and kerosene this is confirmed by the lower rates of heat release. The ignition delay period for LPG is greater than for gasoline and kerosene. Also, θ_{ig}, $\theta_{10\%}$ and $\theta_{90\%}$ for LPG are greater than for gasoline and kerosene. The duration of combustion is 51°, 36° and 33° for LPG, gasoline and kerosene respectively.

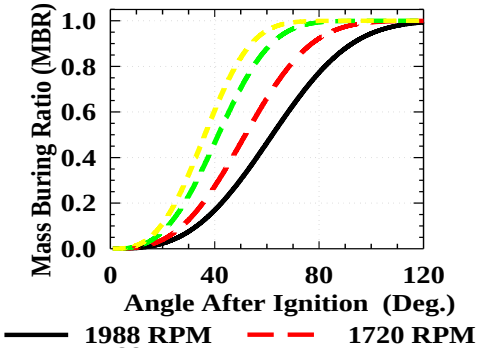

Fig.(29) $m_{burning}$ Using Gasoline for Different Speeds at Full Wide Opening and Stoichiometric Air/Fuel Ratio

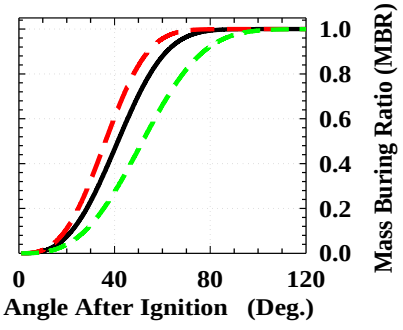

Fig.(30) $m_{burning}$ for Different Fuels at Full Wide Opening and Stoichiometric Air/Fuel Ratio

Gases entropy estimated using the variation of the temperature and pressure as follows:-

$$dS = C_P \ln \frac{T}{T_r} - R \ln \frac{P}{P_r} \qquad (22)$$

$$C_P = R\left(\frac{\gamma}{\gamma - 1}\right), \quad R = \frac{R_u}{M}, \quad M = 29 \qquad (23)$$

Start and end of combustion are determined using entropy change method. So, gases temperature (T), γ(T), C_P(T), and S(T) are calculated using equations (19,12, 22, 23) respectively. Gases entropy versus gases temperature are plotted for different engine speeds and different fuels as shown in the Figs.(31&32). As the compression proceeds from the point of IVC, the gases temperature is stilled lower than the cylinder wall temperature, so, heat transfers from wall to gases and therefore entropy increases. The entropy decreases when the gases temperature exceeded the wall temperature. When the heat release rate due to combustion is higher than the heat transfer rate to the cylinder wall, entropy begins to rise. When the heat transfer rate exceeded the combustion rate, i.e. towards the end of the combustion process, the entropy starts to decrease. So, peak values are achieved at start and end of combustion as shown in Figs (31&32).

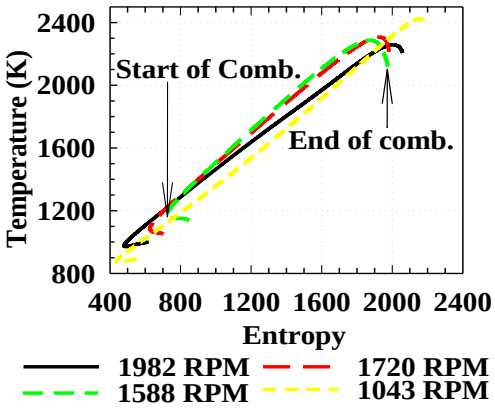

Fig.(31) Entropy Versus Temperature Through Duration of Combustion for Different Engine Speeds

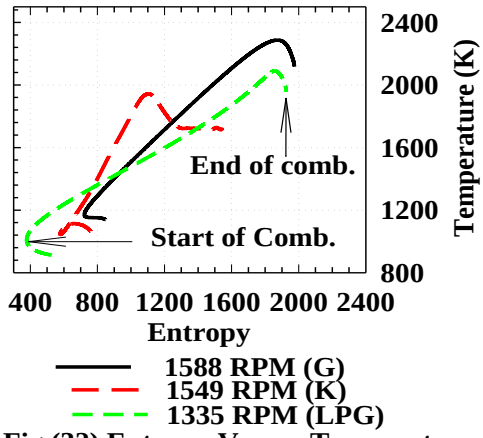

Fig.(32) Entropy Versus Temperature Through Combustion Durations for Different Fuels

An examination of the results indicates that the entropy rises during the combustion process and then starts to decline near the end of combustion. Entropy reaches maximum value very close to the end of combustion and the point of minimum entropy coincided with the beginning of the combustion process. An increase in the engine speed increases the peak value of the entropy at end of combustion. Point of minimum entropy occurs near the start of combustion is not significantly affected by the heat transfer coefficient. This is because the heat transfer is negligible at this condition on account of the low gases temperature. The heat release starts earlier with the increase of engine speed due to increase turbulence and flame stapler near igniter. So, duration of combustion increases with the increase of engine speed. In all operating conditions entropy reaches a minimum during the compression process. So, start and end of combustion are obtained by determining the crank angles at which entropy is minimum or maximum.

Position of peak cylinder pressure, peak gases temperature and peak net heat release versus engine speed are shown in Fig.(33). The results of this figure are obtained from a sequence of figures of engine cylinder pressure, temperature and net heat release at different engine speeds and different fuels used. The position of peak pressure decreases with the increase of engine speed up to 1588 rpm due to increase rate of reaction with the increase of turbulence intensity. After that position of peak pressure increased with the increase of engine speed due to decrease time per cycle. Position of peak heat release traces has the same trend as position of peak pressure. Peak pressure depends mainly on duration of heat release, pressure before ignition, mass and rate of fuel burnt. The position of maximum pressure for gasoline occurred at 10° to 18° CA, for Kerosene at 13° CA and for LPG at 24° CA ATDC for different engine speeds. The positions of maximum heat release rate for gasoline delayed the position of maximum pressure by 30-37°, for kerosene by 15° and for LPG by 17° respectively. The positions of maximum temperature for gasoline delayed the positions of maximum pressure by 20-30°, for kerosene by 16° CA and for LPG by 33°CA respectively. The maximum heat release rate for different fuels and different engine speeds occurred at 48-52% of fuel mass burnt.

Also, combustion duration are determined using different methods as shown in Fig.(34). For different methods, the combustion duration increases with the increase of engine speed. Combustion duration based on fuel mass fraction burned has the smallest duration as CA degree. The difference in combustion duration for the three other methods is small with

respective to each other. The combustion duration is a complex function of turbulence, composition, chemistry, and other factors. Although the turbulence is known to increase with the increase of engine speed, the increase is not thought to be enough to completely compensate for the shorter available times at the higher engine speeds. The dependence on engine speed included assists in accounting for the greater number of crank angles involved in the combustion process as engine speed increases. Duration of combustion is slightly decreased by the increase of pressure at the spark. Actually, an increase in the initial pressure during combustion can greatly alter the way of fuel burns. Higher pressure in a limited volume means higher gases temperature and fuel/air molecules are more reactive. The mixture burns faster, so duration of combustion becomes shorter. The delayed spark firing takes advantage of the more reactive nature of the fuel to get more power output. Under higher inlet pressure, the gases in the cylinder are hotter throughout combustion which is an oxidation reaction, occurs faster. This increase in reaction rate is due to the increase of kinetic energy so it takes a smaller amount of additional energy to reach the activation energy for the reaction.

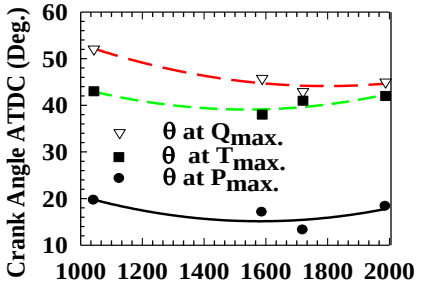

Fig.(33) Positions of $T_{max.}$, $P_{max.}$ and $Q_{max.}$ ATDC for Different Speeds Using Gasoline Fuel

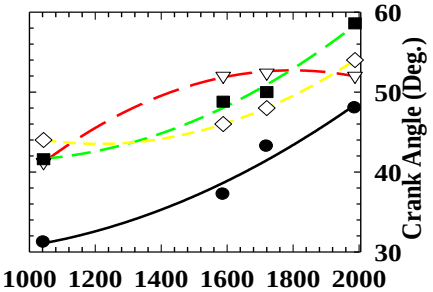

Fig.(34) Duration of Combustion for different methods Using gasoline

Duration of combustion becomes longer as engine speed increases due to the mixture is leaner and the heat release starts earlier. The duration of combustion for LPG is greater than for gasoline and kerosene fuels. This means that, fuel burning rate of kerosene is higher than for gasoline and LPG fuels. For certain mass of fuel burning, the time required for complete combustion of LPG fuel is greater than for gasoline and kerosene fuels respectively. The ignition delay period for LPG is greater than for gasoline and kerosene. Also, θ_{ig}, $\theta_{10\%}$ and $\theta_{90\%}$ for LPG are greater than for gasoline and kerosene. At any crank angle position, percentage of fuel burned for LPG fuel is less than for gasoline and kerosene fuels respectively.

Furthermore, position of start and end of combustion for gasoline fuel based on entropy and γ(T) change with different engine speeds are shown in Fig.(35&36). The start of combustion (SOC) is required for burning rate and heat release analysis. In all cases start of combustion is taken to be the crank angle with the greatest positive rate of change of the measured parameter. The end of combustion (EOC) is required for determining the normalizing value for mass fraction burned and heat release analysis. Position of start and end of combustion based on entropy change and specific heats ratio are good agreement with each other for

different engine speeds. Positions of start and end of combustion as CA increase with the increase of engine speed. When the engine speed increased, more fuel and air are entering combustion chamber, but their ratio is stilled stoichiometric. Therefore start and end of combustion are delayed with increasing engine speeds.

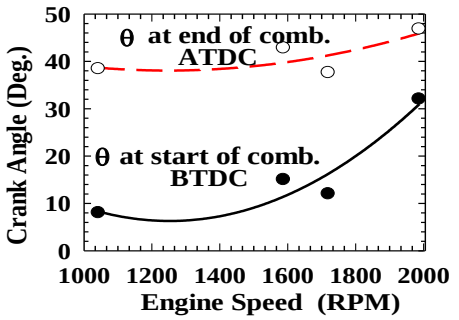

Fig.(35) Crank Angle for Start and End of Combustion for Gasoline Based on Entropy Change

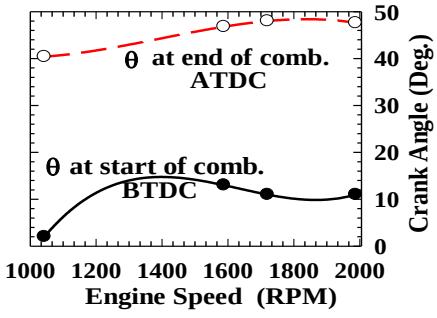

Fig.(36) Crank Angle for Start and End of Combustion for Gasoline Based on Specific Heat Ratio

4. Conclusions

1. Measuring cylinder pressure is very useful tool for analysis heat releases, heat transfer to cylinder walls, entropy change, performance parameters and duration of combustion for different fuels used in SIE.
2. Fast Fourier Transformations (FFT) is a new method for normalizing cylinder pressure in the frequency domain and reconstructing it back to the time domain at different speeds and fuels used. The results demonstrate that the method is easy to use and it provides high accuracy during compression, combustion and expansion processes. Good agreement between the measured and the reconstructed cylinder pressure which demonstrates that the method is applicable for different operating conditions for SIEs.
3. First law-single zone model with γ(T) are accurate and simple method for analysis heat release and heat transfer to cylinder wall. The used of a correct function for γ(T) will bring the exact evaluation of the heat release and heat transfer. As γ(T) decreases, the position of maximum net heat release delays ATDC due to high heat release. Log-Log scale of (V&P) is a good method for determining γ(T) for different speeds and fuels used. A new equation for γ(T) with good agreement with other researchers is obtained using Logarithmic scale of (V&P) as follows:-

$$\gamma = 1.3926 - 1.0718(10^{-4})T - 2.127(10^{-8})T^2 + 1.381(10^{-11})T^3$$

4. The position of peak pressure is earlier than position of peak temperature and heat release for different engine speeds. The position of peak pressure, temperature and heat release for kerosene fuel is earlier than for gasoline and LPG fuels respectively. The position of maximum pressure for gasoline occurred at 10° to 18° CA, for Kerosene at 13° CA and for LPG at 24° CA ATDC for different engine speeds. The positions of maximum heat release rate for gasoline delayed the position of maximum pressure by 30-37°, for kerosene by 15° and for LPG by 17° respectively. The positions of maximum temperature for gasoline delayed the positions of maximum pressure by 20-30°, for kerosene by 16° CA and for LPG by 33°CA respectively. The maximum heat release rate for different fuels and different engine speeds occurred at 48-52% of fuel mass burnt.

5. Duration of combustion for different engine speeds is determined using four different methods: (I) Mass of fuel burned, (II) Change of entropy, (III) Change of specific heats ratio, and (VI) Change of pressure versus cylinder volume in the logarithmic scale. For different methods, duration of combustion increases with the increase of engine speed. Duration of combustion as CA degree based on fuel mass fraction burned is less than other methods. The other three methods are good agreement with each other for different engine speeds. The duration of combustion for kerosene is smaller than for gasoline and LPG respectively.

References

1. Pin Zeng, Robert G. Prucka, Zoran S. Filipi And Dennis N. Assanis, (2004) " Reconstructing Cylinder Pressure of a Spark-Ignition Engine for Heat Transfer and Heat Release Analyses" ASME Internal Combustion Engine Division Fall Technical Conference , October 24-27, Long Beach, CA, USA.
2. Nicholas M Brown, "Characterization of Emissions and Combustion Stability of a Port Fuelled Spark Ignition Engine" PhD thesis, University of Nottingham, 2009.
3. Kamin ski T., Wendeker M., Urbanowicz K., and Litaka G., 2004, "Combustion Process in a Spark Ignition Engine: Dynamics and Noise Level Estimation", American Institute of Physics, June, Volume 14, Number 2.
4. Eriksson Lars and Andersson Ingemar, 2002, "An analytic model for cylinder pressure in a four stroke SI engine", Society of Automotive Engineers, Inc.
5. Marcus Klein, 2004, "A Specific Heats Ratio Model and Compression Ratio Estimation", Division of Vehicular Systems Department of Electrical Engineering, Linköping Studies in Science and Technology Thesis No. 1104.
6. Abu-Nada E., Al-Hinti I., Al-Sarkhi A. and Akash B., 2006, "Thermodynamic modeling of spark-ignition engine: Effect of temperature dependent specific heats" International Communications in Heat and Mass Transfer, December, Volume 33, Issue 10, Pages 1264-1272.
7. Lanzafame R. and Meaana M., 2003, "ICE Gross Heat Release Strongly Influenced By Specific Heats Ratio Values", International Journal of Automotive Technology, Vol. 4, No. 3, pp. 125-133.
8. Jorge J.G. Martins, Bernardo S. Ribeiro and Ion V. Ion, 2009, "Thermodynamic analysis of Spark Ignition engines Using the Entropy Generation Minimization method", Int. J. Energy, Vol. 6, No. 1.
9. Bernardo Ribeiro, Jorge Martins and António Nunes, 2007, "Generation of Entropy in Spark Ignition Engines", Int. Journal of Thermodynamics, June, ISSN 1301-9724 Vol. 10 (No. 2), pp. 53-60.
10. Mohand, Tazerout and Ramesh A., 2000, "A New Method to Determine the Start and End of Combustion in an Internal Combustion Engine Using Entropy Changes", International Journal Applied Thermodynamics, Vol.3, (No.2), pp.49-55, ISSN 1301-9724.
11. Sotiris Gritsis, 2001, "Internal Combustion Engine Intake Acoustics", MSc Thesis, Canfield Universit.
12. Heywood, (1988), "Internal combustion engine fundamentals", Megraw-Hill institute.
13. Brunt, M. F. J., Rai, H. and Emtage, A. L., "The calculation of heat release energy from engine cylinder pressure data", SAE, Paper 981052.
14. Woschni, G., 1967, "Universally Applicable Equation for the Instantaneous Heat Transfer Coefficient in the Internal Combustion Engine", SAE Paper 670931.

15. Gatowski A.J., Balles E. N., Chun M.K., Nelson E.F., Ekchian A.J., and Heywood B.J, 1984, "Heat Release Analysis of Engine Pressure Data", SAE Technical Paper 841359.

Nomenclatures

ABDC	after bottom dead center
ATDC	after top dead center
B	cylinder bore diameter, m.
BDC	bottom dead center
CAD	crank angle degree, deg
C_P	specific heat at constant pressure, J/kg
EOC	K
EVO	end of combustion, (deg)
EVC	exhaust valve open
G	exhaust valve closed
h_C	gasoline
IVC	heat transfer coefficient, W /m^2K
IVO	inlet valve closed
K	inlet valve opened
L	kerosene
L_{cr}	engine stroke, m
L_{ct}	connecting rod length, m
LPG	crank radius, m
TDC	liquefied petroleum gas
R	top dead center
m	gas constant, J/kg K
	mass, kg
mfb	mass fuel burnt, %
M	molecular weight
N	engine speed, RPM
P	pressure, P_a
SO	start of combustion, (deg)
C	entropy, J/kg K
S	spark ignition engine
SIE	mean piston speed, m/s
S_p	temperature, K
T	clearance volume, m^3.
V_c	displacement volume, m^3
V_d	total engine volume, m^3
$V_{eng.}$	heat released, J
Q	heat transfer rate, j/s
$\dot{Q}_W$	charge velocity, m/s
W	piston displacement, m
Z	**Greek letters**
	angle, (deg.)
θ	duration of combustion (deg)
$\Delta\theta$	air density, kg/m^3.
ρ_{air}	specific heat ratio
γ	